0273-2289/02/101/0211/$14.25

Scale-Up of Microbubble Dispersion Generator for Aerobic Fermentation

P. Hensirisak,[1] P. Parasukulsatid,[1] F. A. Agblevor,*,[1] J. S. Cundiff,[1] and W. H. Velander[2]

[1]Biological Systems Engineering Department and [2]Department of Chemical Engineering, Virginia Polytechnic Institute and State University, Blacksburg, VA 24061, E-mail: fagblevo@vt.edu

Received July 2001; Revised December 2001; Accepted January 2002

Abstract

A laboratory-scale microbubble dispersion (MBD) generator was shown to improve oxygen transfer to aerobic microorganisms when coupled to the conventional air-sparger. However, the process was not demonstrated on a large scale to prove its practical application. We investigated the scale-up of a spinning-disk MBD generator for the aerobic fermentation of *Saccharomyces cerevisiae* (baker's yeast). A 1-L spinning-disk MBD generator was used to supply air for 1- and 50-L working volume fermentation of baker's yeast. For the two levels investigated, the MBD generator maintained an adequate supply of surfactant-stabilized air microbubbles to the microorganisms at a relatively low agitation rate (150 rpm). There was a significant improvement in oxygen transfer to the microorganism relative to the conventional sparger. The volumetric mass transfer coefficient, k_La, for the MBD system at 150 rpm was 765 h^{-1} compared to 937 h^{-1} for the conventional sparger at 500 rpm. It is plausible to surmise that fermentation using larger working volumes may further improve the k_La values and the dissolved oxygen (DO) levels because of longer hold-up times and, consequently, improve cell growth. There was no statistically significant difference between the cell mass yield on substrate (0.43 g/g) under the MBD regime at an agitation rate of 150 rpm and that achieved for the conventional air-sparged system (0.53 g/g) at an agitation rate of 500 rpm. The total power consumption per unit volume of broth in the 50-L conventional air-sparged system was threefold that for the MBD unit for a similar product yield. Practical application of the MBD technology can be expected to reduce power consumption and therefore operating costs for aerobic fermentation.

*Author to whom all correspondence and reprint requests should be addressed.

Index Entries: Microbubble; fermentation; aeration; *Saccharomyces cerevisiae*; power consumption.

Introduction

The achievement of high oxygen mass transfer rate with minimal power input and relatively low shear is a major challenge in aerobic bioreactor design. The conventional stirred-tank bioreactor can achieve very high mass transfer rates but at the risk of increased shear, which may be detrimental to some microorganisms. Unlike soluble nutrients such as glucose, ammonia, xylose, and most salts, the solubility of oxygen in water is very low, but the utilization rate is very high. The situation is further exacerbated by the lowering of solubility of oxygen in water in the presence of dissolved salts. For laboratory-scale fermentation, oxygen requirements can be readily met by using shaker baths. However, as the volume of the reactor increases, the cost of supplying sufficient oxygen for effective cell growth and fermentation becomes very high. Large-scale aerobic cultures, 10,000 L or larger, are oxygen mass transfer limited. Gas–liquid interfacial surface area and bubble residence time phenomena are the limiting factors for oxygen delivery to the microorganisms. Gas–liquid surface area can be manipulated by changing interfacial tension, but this factor is difficult to adjust.

The conventional method of increasing dissolved oxygen level in a fermentation broth has been to increase the agitation speed, increase gas flow rate, or increase the oxygen partial pressure *(1)*. Kaster et al. *(2)*, Bredwell et al. *(3)*, and Srivastava et al. *(4)* found that the mass transfer rate of oxygen in fermenters was enhanced when sparged with microbubble dispersions (MBD). The major advantage of this system was the enhanced mass transfer at very low agitation rates because of the increased interfacial surface area provided by the microbubbles. Furthermore, the decreased bubble size enhanced the gas hold-up in the reactor because of slower bubble-rise velocities.

One type of MBD design uses a spinning disk to generate a mixture of colloidal gas aphron (CGA)-sized bubbles (20–70 µm) and some large bubbles (3–5 mm) *(5)*. The CGAs have special properties because of the very small size of the bubbles, and the type of surface that surrounds each aphron. In the presence of surfactants, the coalescence of microbubbles is hindered by electrical repulsive forces on the surface, which act as energy barriers *(6)*. Because of these unusual properties, CGAs are markedly different from ordinary bubbles *(7)*. The CGA-sized bubbles rise very slowly against the influence of gravity, and scarcely, if ever, coalesce as long as they are completely immersed in a surfactant *(5)*.

The application of the MBD to aerobic yeast fermentation was investigated by Kaster et al. *(8)* in a stirred-tank reactor. The micron-sized bubbles generated were stabilized by the natural surfactants in the yeast fermentation broth *(9,10)*. The microbubble dispersions consisting of surfactant-stabilized bubbles with diameters 20–1000 µm were sparged into a 2-L

fermenter during the fermentation of *Saccharomyces cerevisiae*. Compared to bubbles delivered by a conventional sparger (3–5 mm diameter), the microbubbles provided larger interfacial area for oxygen transport and longer gas hold-up because of their comparatively slow rise in the fluid. The microbubble dispersion provided efficient oxygen transfer with k_La values 30% greater than conventional sparged air at equivalent agitator power to volume ratios *(2)*.

Although the microbubble dispersion showed a considerable improvement in oxygen transfer rate on the laboratory scale, it was not evaluated for large-scale fermentation *(2)*. In these small-scale experiments, the power input per volume of broth (P/V) can be significantly higher than the power input per volume of broth in an industrial-scale fermenter. For example, the P/V values in streptomycin production were reported to be in the range of 0.0010 to 0.0150 hp/gal for 5-L laboratory fermentation, while in the 15,000-gal fermentation, the P/V were found to be from 0.0007 to 0.0041 hp/gal *(11)*. Thus, the microbial growth kinetics observed in laboratory-scale experiments often do not agree with the kinetics observed in large-scale fermentation. The disagreement can be attributed to various effects such as the changes in mixing pattern, and mass and heat transfer rates. Microbial properties such as growth, adaptation, and shear sensitivity can also complicate the scale-up. Therefore, experiments are needed to demonstrate the applicability of the microbubble dispersion technology to industrial-scale reactor where P/V ratios are much smaller.

Saccharomyces cerevisiae was selected as the model aerobic organism in our experiments because:

1. It is relatively insensitive to shear.
2. It is important in the food and beverage industry.
3. Its overall metabolism is simple, the only major products are yeast cells, ethanol, and carbon dioxide.
4. It can be easily grown in culture because of its highly competitive growth characteristics, which outcompete contaminating microorganisms.

In this study, the 1-L spinning disk microbubble dispersion generator volume was fixed while the fermenter working volume was scaled-up to 50 L. Our overall goal was to investigate the scale-up of this technology for industrial aerobic fermentation.

Materials and Methods

Organism and Inoculum Preparation

The microorganism used in this study, *Saccharomyces cerevisiae* ATCC 4111, was obtained from the American Type Culture Collection (Manassas, VA). The lyophilized culture was rehydrated in yeast malt (3 g yeast extract, 3 g malt extract, 5 g peptone, and 10 g dextrose) liquid medium and incubated for 18 h at 37°C. Stock culture was maintained on a Difco yeast malt

(YM) agar medium at 4°C and subcultured every month to maintain viability. Starter culture was prepared by transferring two loops of the stock culture into a 500 mL Erlenmeyer flask containing 150 mL of sterilized standard YM broth (21 g YM per liter of distilled water) and incubated on a rotary shaker at 200 rpm for 18 h at 30°C.

Air-Sparged Fermentation

One-Liter Fermenter

The 1-L working volume fermentation was conducted in a 1.6-L benchtop Bioflo III fermenter (New Brunswick Scientific, NJ). The fermenter was equipped with pH, dissolved oxygen, temperature, and foam probes controlled by a proportional/integral/derivative (PID) controller. The addition of acids, bases, antifoam, and nutrients were controlled from the module. The fermenter was filled with 1 L YM broth solution (concentration 21 g/L) and the pH probe was calibrated before sterilization. The dissolved oxygen (DO) and pH probes, cooling water, condenser water, and agitator were disconnected from the module and the entire reactor assembly was sterilized at 121°C for 25 min in an AMSCO sterilizer (Steris Corporation, Hicksville, NY). After sterilization, about 200 mL of sterilized makeup water was added through the media port to restore the medium volume to 1.0 L. The medium was cooled to 35°C and both the DO and pH probes were recalibrated.

The medium was inoculated with 49 mL of starter culture (concentration 8.5 g/L). Fermentation was carried out at 35°C, pH 6, atmospheric pressure, and agitation rate was varied according to the fermentation regime (144 or 476 rpm). A constant pH was maintained by periodic automatic addition of 1.0 *M* NH_4OH or 0.5 *M* HCl. Air flow rate was fixed at 100 mL/min (equivalent to 0.1 volume of air per volume of medium per minute or 0.1 vvm). The DO level was not controlled but was allowed to fall freely until equilibrium level was established.

Aliquots were taken every hour for 24 h. Cell mass concentrations were measured spectrophotometrically at 620 nm using Spectronic 1001 instrument (Milton Roy Company, Rochester, NY). Glucose contents of the aliquots were measured by the dinitrosalicylic acid method *(12)* and DO levels were recorded manually every hour.

Seventy-Two-Liter Fermenter

The scale-up fermentations were run in a 72-L pilot-scale fermenter (BIOSTAT® U 50, B. Braun Biotech Inc., Allentown, PA) at a working volume of 50 L. Unlike the Bioflo III fermenter, this unit was sterilized in place and air was injected through the bottom of the vessel via a sparger with 1-mm-diameter orifices. Before filling the vessel with the fermentation medium, the pH electrode was calibrated with calibration buffers. The fermenter was filled with fermentation medium (21 g/L YM broth) to a vol 50 L and the automatic sterilization cycle was operated. The medium was then cooled to 35°C and the pH and DO probes were recalibrated.

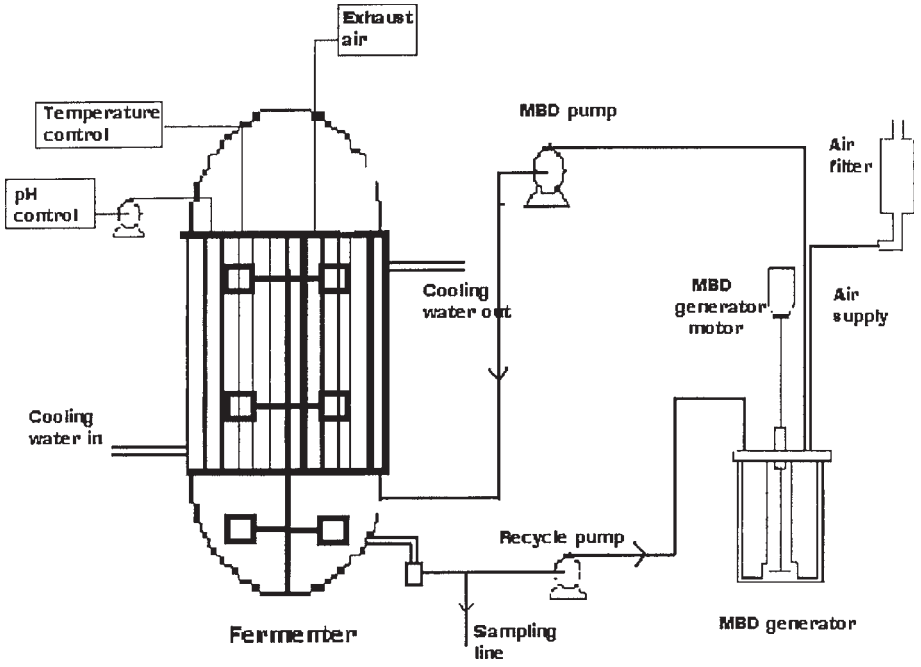

Fig. 1. The experimental set-up of fermenter and MBD generator in pilot-scale experiment.

Because the objective of these series of experiments was to scale-up the results for the 1-L fermenter, the Hubbard scale-up method *(13,14)* was used to determine the air flow and agitation rates. In the Hubbard approach, the scale-up is based on a constant $k_L a$ value in both reactors. Thus, the air flow rate was set at 5 L/min (0.1 vvm) for the 50 L working volume. The agitation rates were set at 150 and 500 rpm depending on the fermentation regime. The fermentation were similar to those for the 1.6-L fermenter. DO levels were continuously monitored with Ingold electrode (Mettler Toledo Inc, Columbus, OH). Data recording, sampling, and aliquot analyses were similar to the protocols used for the 1.6-L fermenter.

MBD Sparged Fermentation

The MBD were produced using a spinning-disk apparatus first described by Sebba *(5)*. The schematic diagram of the apparatus is shown in Fig. 1. The system consisted of a high-speed electric motor that spun a 5-cm-diameter by 1-cm-thick stainless-steel disk at speeds up to 4000 rpm. Stationary baffles located 5 mm from the spinning disk created localized high-shear zones. The stainless-steel disk and baffles were mounted in a 1-L vessel that contained recirculated fermentation broth. Two peristaltic pumps were connected to the unit to recycle the fermentation broth and transfer the MBD to the reactor.

The spinning disk was located 2–3 cm below the surface of the fermentation broth. When it spun, strong waves were generated, which struck the baffles, sheared the large air bubbles created, and the entrained the microbubbles. The natural surfactant in the fermentation broth stabilized the microbubbles generated. In our experiment, no external surfactant was added to the MBD vessel. Instead, a small fraction of the fermentation broth was circulated through microbubble generator as a source of natural surfactant.

Fermentation

The MBD-sparged fermentation procedures for the 1.6-L and the 72-L fermenters were similar to those described above for the air-sparged fermentation. However, instead of sparging the air directly into the fermenter as practiced in the air-sparged reactor, the air stream was routed through the MBD generator where it was converted into MBD before sparging.

For the 1.6-L fermenter, the MBD vessel was initially filled with 200 mL of YM broth, and the entire unit was sterilized in an autoclave at 121°C for 15 min. The MBD unit was connected to the Bioflo III fermenter as shown in Fig. 1. A peristaltic recycle pump was used to transfer fermentation broth to the MBD vessel at 40 mL/min. Air at 100 mL/min was introduced into the MBD vessel and the stainless-steel disk was spun at 4000 rpm to create the MBD. The MBD was transferred at 100 mL/min by a peristaltic pump to the ring sparger in the fermenter. A six-blade disk turbine impeller at similar agitation rates as the air-sparged fermenter (144 and 476 rpm) was used to disperse the MBD.

The setup for the 72-L fermenter was similar to that described for the air-sparged fermentation. The same MBD unit used for the 1.6-L fermenter was used for this unit. The setup of the MBD unit was similar to that for the 1.6-L unit. The differences between the two units were in the air flow rates, MBD flow rate, and fermentation broth flow rate. For the 50-L working volume, the air flow rate into the microbubble generator was 5 L/min and MBD was transferred at 5 L/min to the sparger ring and dispersed into the fermentation medium. The fermentation broth was recycled at 1.1 L/min.

The fermentation broth was sampled at similar intervals as those for the air-sparged fermentation. All samples were analyzed for cell mass and glucose concentrations. DO levels were not controlled but were allowed to fall freely until equilibrium was established.

Assays

Cell Mass Concentration

Biomass concentration (g/L) was determined from the optical density (OD) measurement at 620 nm on a Spectronic 1001 spectrophotometer. After the OD values were measured, the samples were transferred into 10-mL centrifugal tubes and centrifuged at 11,000*g* for 10 min. The cells were decanted, washed, recentrifuged, and decanted. The washed samples were dried at 80°C for 24 h to a constant mass and weighed. The OD and

gravimetric data were used to develop a calibration curve for all the runs. When OD values exceeded 0.8 absorbance unit, the sample was diluted to fit the calibration range and the cell mass concentration was multiplied by the dilution factor.

Glucose Concentration

The glucose concentration of the fermentation broth was determined by the dinitrosalicylic acid (DNS) method *(12)*. In this method, DNS reagent was prepared from Rochelle salt, 306 g; phenol, 8.13 g; sodium metabisulfite, 8.3 g; phenolphthalein, 3 mL; NaOH, 19.8 g; and 0.1 *N* HCl. Standard glucose solutions were prepared in concentrations of 0.2, 0.4, 0.6, 0.8, and 1.0 g L^{-1}. One milliliter of standard glucose solution was pipeted into a test tube and 3 mL of DNS reagent was added. The mixture was placed in boiling water for 5 min to develop color and then cooled to room temperature. About 2 mL of the sample was placed in a cuvet and the absorbance at 550 nm was measured. Deionized water was used as reference. To determine the glucose concentration in the fermentation broth, samples (1.5 mL) were centrifuged at 11,000*g* for 10 min and decanted. The glucose content of the supernatant solution was measured by the DNS method using the glucose calibration curve developed above.

Determination of k_La Values

The volumetric oxygen transfer coefficient (k_La) was determined by the yield coefficient method *(15)*. This method is based on the assumption that at steady state, the oxygen uptake rate by the cells is equal to the oxygen transfer rate. Thus, the k_La value was calculated from Eq. 1:

$$k_La = \frac{\mu X (K'/Y_O)}{(C^* - C)} \quad (1)$$

where k_La = volumetric oxygen transfer coefficient (h^{-1}), μ = specific growth rate (h^{-1}), X = cell mass (g L^{-1}), K' = conversion factor = 31.25 (mmol O_2 g O_2^{-1}), Y_O = yield coefficient on oxygen (g cell mass g O_2^{-1}), C* = saturated dissolved oxygen concentration (0.19 mmol O_2 L^{-1}), and C = dissolved oxygen concentration (mmol O_2 L^{-1}).

The yield coefficient on oxygen was determined from the correlation of Mateles *(16)*. The yield coefficient on substrate was determined for each batch experiment and then the Mateles correlation of $1/Y_s$ vs $1/Y_O$ was used to determine Y_O. The maximum specific growth rate was determined from the log phase of each batch run. The dissolved oxygen concentration (C) was determined from the DO value (% saturation dissolved oxygen) interpolated with the DO value at 100%. For YM broth solution at 35°C and pH 6, the 100% DO was 0.19 mmol O_2 L^{-1}.

Power Measurement

Impeller power: The power consumption of ungassed Newtonian fluids can be characterized by a dimensionless power number (N_p) defined as the

ratio of external force to the inertia force exerted by the fluid. The power number can be determined from Eq. 2 *(17)*:

$$N_p = P_0/(N^3D^5\rho) \tag{2}$$

where P_0 is the power supplied to the agitator, N is the rotational speed of the impeller, D is the diameter of the impeller, and ρ is the density of the fluid. Thus, for a given fluid system, the power number will depend on the geometry and power of the agitator. The power for ungassed system can be expressed as:

$$P_0 = N_p\rho N^3D^5 \tag{3}$$

In an agitated system, the fluid flow is characterized by Reynolds number (Re):

$$\mathrm{Re} = ND^2\rho/\mu \tag{4}$$

where μ is the viscosity.

Studies have shown that for gassed systems, the presence of the gas bubbles affects the power consumption. The gas bubbles reduce the density of the fluid and this results in the reduction in power consumption. The system under consideration is a gas–liquid dispersion, so in order to measure the power consumed, the ungassed model has to be modified. For aerated systems, Oyama and Endoh *(18)* developed a correlation between the gassed and ungassed power consumption using the aeration number (N_a) as shown in Eq. 5:

$$P_g/P_0 = N_a = (f_1 \times Q)/ND^3 \tag{5}$$

where P_g = gassed power (W), P_0 = ungassed power (W), N_a = aeration number (dimensionless), f_1 = function given graphically, Q = volumetric gas flow rate (L s^{-1}), D = impeller diameter (cm), and N = impeller speed (rev s^{-1}). To determine the power consumption in a gassed system the power number for the ungassed system was determined from the correlation between the Reynolds number and the power number according to McCabe et al. *(17)*. The power (P_g) consumption in the gassed system was then determined from Eq. 5 using the correlation developed by Oyama and Endoh *(18)*.

Microbubble generator power consumption: The power consumption in the MBD generator system included the power of the motor, the MBD delivery pump, and the MBD recycling pump as shown in Eq. 6:

$$\mathrm{P_{MBD}} = \mathrm{P_{motor}} + \mathrm{P_{MBD\ pump}} + \mathrm{P_{recycle\ pump}} \tag{6}$$

$$\mathrm{P_{motor}} = \mathrm{current} \times \mathrm{voltage} \tag{7}$$

The power for the MBD delivery and recycle pumps was calculated from the steady-state macroscopic mechanical energy balance *(19)*:

$$\Delta\frac{1}{2}\langle v\rangle^2 + g\Delta h + \int_{p_1}^{p_2}\frac{1}{\rho}\,dp + W + \sum_i\left(\frac{1}{2}\langle v\rangle^2\frac{L}{D}f\right)_i + \sum_i\left(\frac{1}{2}\langle v\rangle^2 e_v\right)_i = 0 \tag{8}$$

where $\langle v \rangle$ is the average velocity of the fluid, Δh is the height through which the fluid was lifted, L is length of pipe, D is the diameter of pipe, e_v is the friction loss due to fittings, f is the friction factor in the straight pipe, Δp is the pressure drop across the pipe line, and W is the shaft work by the pump.

Air Compressor Power Consumption

The air compressor power consumption was estimated from the following correlation:

$$H_p = 0.0154\ QpX \tag{9}$$

where H_p is the power (hp), Q is the fluid flow rate (ft^3/min), p is the pressure (psi), and X is a correlation factor according to Perry and Chilton *(20)*.

Results and Discussions

The goal of the MBD technology development is to increase oxygen transfer at low agitation rate to growing microorganisms in a stirred-tank reactor. Attaining this goal will decrease the operating cost of aerobic fermentation processes, because a large fraction of the process cost is associated with power requirements for agitation. The microbubble size and bubble stability were not determined in these experiments because they were measured for this apparatus by Kaster et al. *(2)*.

One-Liter Fermentation

The effectiveness of the MBD was based on the relative improvement in volumetric mass transfer rate and microbial growth rate. Effective oxygen transfer in an aerobic fermentation system can be indicated by the volumetric oxygen transfer coefficient (k_La) and by the pattern of product formation. In the aerobic fermentation of baker's yeast (*S. cerevisiae*), the cell mass was the desired product; thus, the growth pattern, growth yield, and specific growth rate of *S. cerevisiae* were studied for batch fermentations using air sparging and MBD sparging. The growth patterns and dissolved oxygen profile for the two agitation speeds using air and MBD sparging are shown in Fig. 2.

The dry cell mass concentration profile of the 144-rpm agitation speed showed that there was more biomass accumulation using the MBD sparging than the air sparging. Whereas the stationary phase biomass concentration in the MBD-sparged fermentation was 3.82 ± 0.14 g/L, that in the air-sparged system was 2.54 ± 0.08 g/L (Table 1). The difference in biomass concentrations for the two systems was statistically significant ($p < 0.05$). The dissolved oxygen profile for these runs showed that the oxygen limitation for the air-sparged system was more severe than the MBD-sparged system (Fig. 2). Shuler and Kargi *(21)* reported that if oxygen was the rate-limiting factor, the specific growth rate would vary with the dissolved oxygen concentration according to saturation kinetics. Above some critical oxygen concentration, the specific growth rate would be independent of

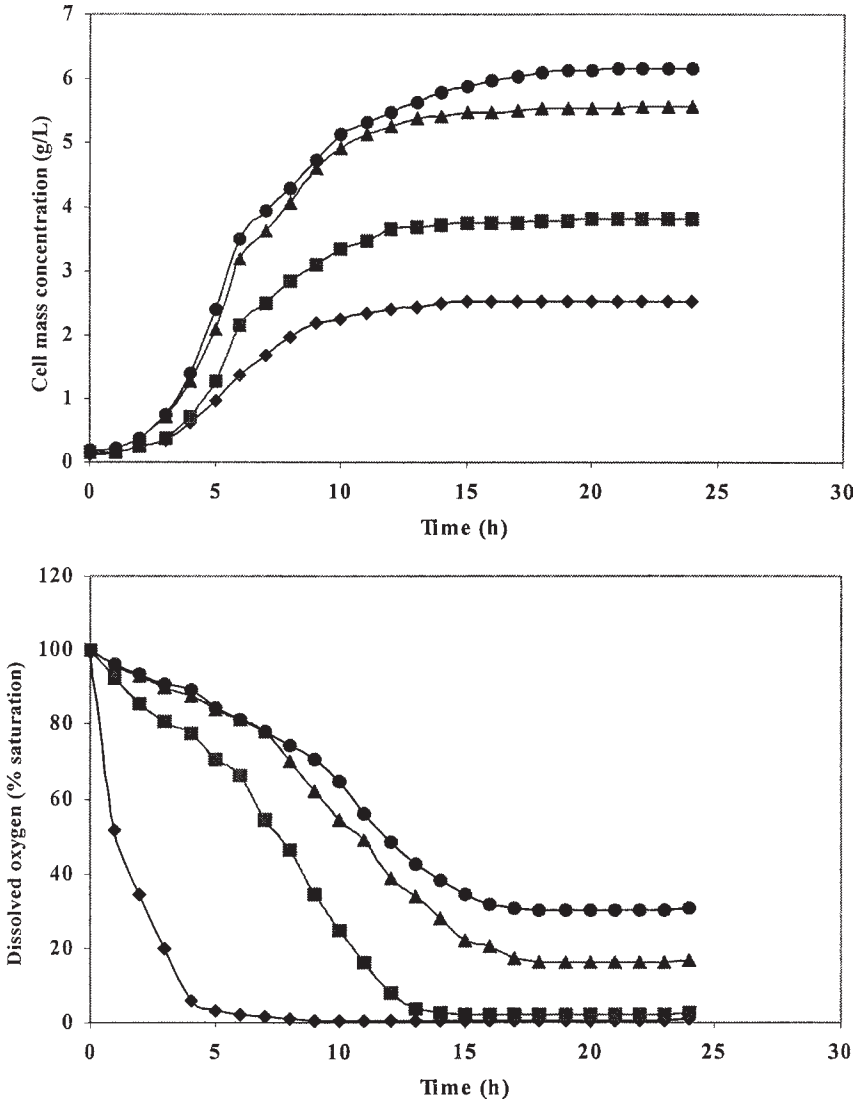

Fig. 2. Comparison of yeast growth profiles and oxygen profiles in 1-L fermenter. 144 rpm agitation, air sparging (◆), 144 rpm agitation, MBD sparging (■), 476 rpm agitation, air sparging (▲), and 476 rpm agitation, MBD sparging (●).

the dissolved oxygen concentration *(22)*. The dissolved oxygen concentration for our fermentations followed the saturation kinetics (Fig. 3A, B) showing that oxygen was the limiting substrate. The critical dissolved oxygen for this yeast was 5% of the saturated dissolved oxygen concentration, which was in agreement with Shuler and Kargi. The maximum specific growth rate was determined by the Hanes–Woolf plot (Fig. 3B) as 0.57 h^{-1} and the saturation constant was 0.51% DO *(23)*.

For the fermentation at 144 rpm, both the MBD-sparged and the air-sparged dissolved oxygen concentrations were below the critical concen-

Table 1
Cell Mass Concentration, Saturation Dissolved Oxygen Concentration, Cell Mass Yield, Specific Growth Rate, and Volumetric Oxygen Transfer of 1-L and 50-L Fermentations

Reactor volume (L)	Air supply	N^a (rpm)	X^b (g/L)	DO[c] (%)	Y_s^d (g/g)	μ^e (1/h)	k_La^f (1/h)
1.6	Air sparger	144	2.54 ± 0.08	0.3 ± 0.05	0.27 ± 0.01	0.47 ± 0.02	338.77 ± 11.0
1.6	MBD	144	3.82 ± 0.14	2.2 ± 0.16	0.40 ± 0.02	0.52 ± 0.01	682.03 ± 0.58
1.6	Air sparger	476	5.56 ± 0.12	16.0 ± 1.17	0.60 ± 0.01	0.53 ± 0.02	800.57 ± 4.13
1.6	MBD	476	6.17 ± 0.12	30.1 ± 0.40	0.66 ± 0.01	0.56 ± 0.01	990.24 ± 1.68
72	Air sparger	150	2.46 ± 0.11	1.3 ± 0.26	0.26 ± 0.02	0.39 ± 0.01	407.00 ± 2.34
72	MBD	150	4.22 ± 0.18	5.4 ± 0.14	0.43 ± 0.02	0.52 ± 0.01	765.18 ± 4.05
72	Air sparger	500	5.08 ± 0.07	20.8 ± 0.45	0.53 ± 0.01	0.56 ± 0.01	937.14 ± 1.92
72	MBD	500	5.57 ± 0.08	30.0 ± 0.21	0.59 ± 0.01	0.59 ± 0.01	1089.10 ± 2.29

[a]N = agitation speed.
[b]X = cell mass concentration.
[c]DO = dissolved oxygen concentration (% saturation).
[d]Y_s = cell mass yield, no unit (g cell mass/L/g substrate/L).
[e]μ = specific growth rate.
[f]k_La = volumetric oxygen transfer coefficient.

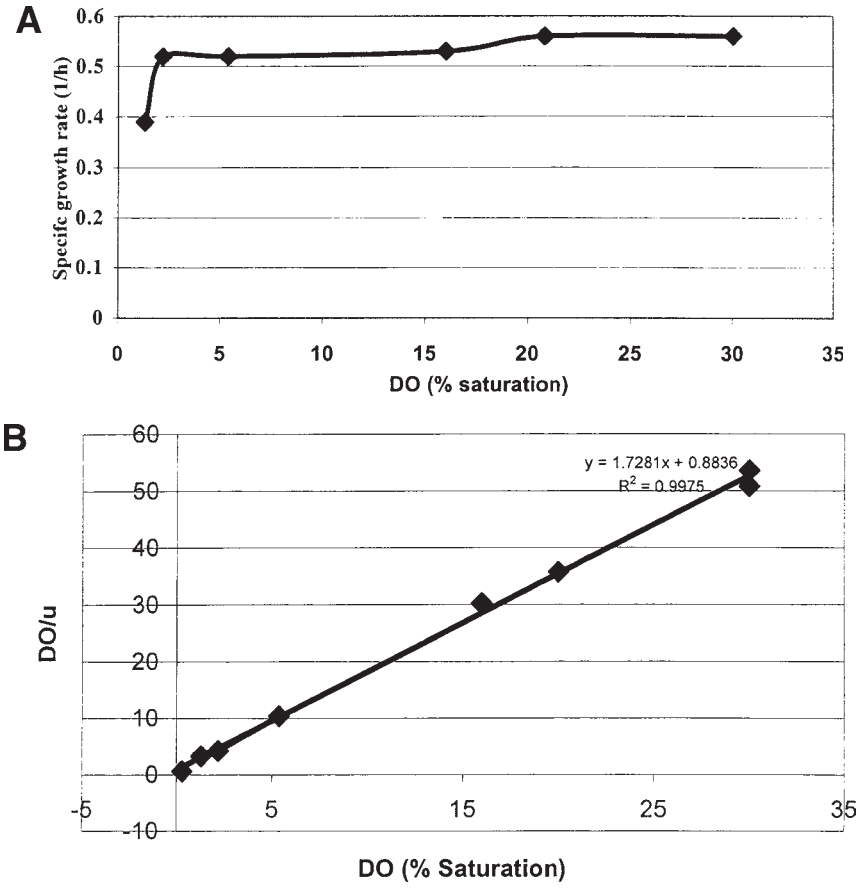

Fig. 3. **(A)** The effect of dissolved oxygen concentration on the specific growth rate of *Saccharomyces cerevisiae*, showing the saturation kinetics. **(B)** The Hanes–Woolf plot of the dissolved oxygen concentration in the fermentation broth.

tration, thus, there was growth limitation. It can be seen that the MBD improved the dissolved oxygen concentration for the broth because of the improved oxygen mass transfer rate because of the larger interfacial surface area.

The values for the volumetric oxygen transfer rate k_La were calculated by the yield coefficient method, using the amount of yeast produced per gram of glucose consumed to calculate the amount of oxygen consumed. The k_La value for the MBD-sparged system was 682 h^{-1} compared to 338 h^{-1} for the air-sparged fermentation, clearly showing that the microbubble influenced the oxygen mass transfer rate.

When the fermentation was carried out at a higher agitation rate at a constant airflow rate of 0.1 vvm, the specific growth rate increased for both the MBD-sparged and the air-sparged fermentations. Cell mass concentrations in both systems increased above those observed for the fermentations at 144 rpm (Fig. 2). The MBD-sparged fermentation broth had a higher

oxygen concentration than the corresponding air-sparged system as shown by the dissolved oxygen profiles for the two systems. In both cases, the dissolved oxygen concentration was above the critical value of 5% of the saturation value and therefore the specific growth rates were similar. The differences in the stationary phase cell mass concentrations were also small, 5.56 ± 0.12 g/L and 6.17 ± 0.12 g/L, respectively, for the air-sparged and the MBD-sparged. The observed cell mass yields were similar, 0.60 g/g and 0.66 g/g, respectively, for the air-sparged and the MBD-sparged fermentations (Table 1). In both systems, there was improvement in the oxygen volumetric mass transfer rate (Table 1).

50-Liter Fermentation

The scale-up to 50 L working volume using the Hubbard methodology *(13,14)* clearly showed the positive attributes of the MBD-sparged system. Using the Hubbard methodology, the equivalent minimal agitation rate at the 50-L working volume was 150 rpm instead of the 144 rpm used in the 1-L working volume. The cell mass growth profiles showed a higher dry cell mass concentration in the stationary phase for the MBD-sparged compared to the air-sparged system (Fig. 4). The dry cell mass concentration at the stationary phase for the air-sparged system in the 50-L fermentation (2.46 g/L) was similar to that obtained in the 1-L working volume (2.54 g/L). However, for the MBD-sparged fermentation, the dry cell mass concentration at the stationary phase in the 50-L fermentation (4.22 g/L) was higher than that in the 1-L fermentation (Table 1). The saturation dissolved oxygen profiles showed that whereas the MBD-sparged system dissolved oxygen exceeded the critical concentration for the yeast, that of the air-sparged system was below the critical concentration (Fig. 3A). Because the DO level for the MBD-sparged system was high, the specific growth rate approached the maximum for this microorganism. On the contrary, the specific growth rate for the air-sparged system was below the maximum, hence there was lower biomass accumulation. These trends were also corroborated by the growth yield on substrate (Table 1). There was also significant difference in the volumetric oxygen transfer coefficient. The $k_L a$ values were 407 h^{-1} and 765 h^{-1}, respectively, for the air-sparged and MBD-sparged fermentations. It appears the improved oxygen mass transfer in the larger fermenter was probably because of the longer residence times of the microbubbles in the fermenter. Whereas in the 1 L working volume, the airflow rate was the same, the volume of the liquid was less and therefore the path traversed by the microbubble was less than that encountered in the 50-L fermentation. It is plausible to surmise that fermentation using larger working volumes may further improve the $k_L a$ values and the DO levels because of longer hold-up times and consequently improve cell growth.

When the agitation rate was increased to 500 rpm at the constant airflow rate of 0.1 vvm, the dry cell mass concentration in the stationary phase increased. The difference between the cell concentrations in the air-sparged and MBD-sparged fermentations was insignificant (Table 1). The specific

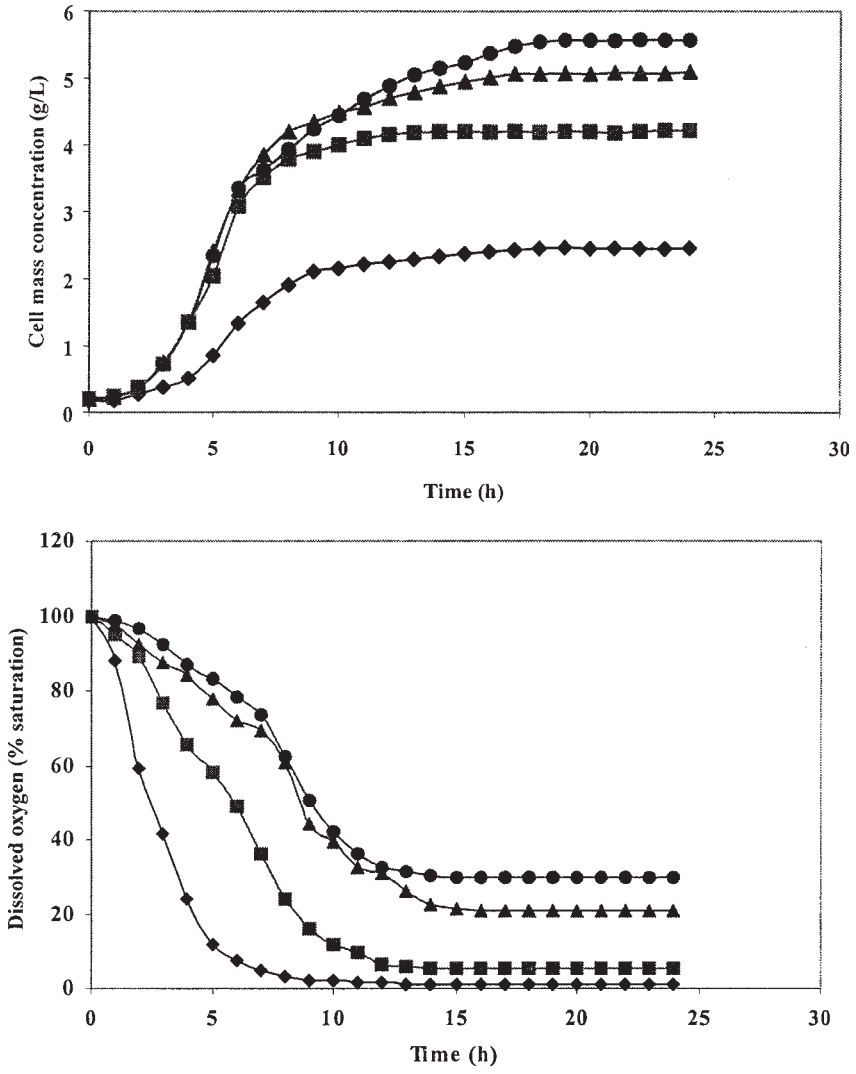

Fig. 4. Comparison of yeast growth profiles in 50-L cell cultivation. 150 rpm agitation, air sparging (◆), 150 rpm agitation, MBD sparging (■), 500 rpm agitation, air sparging (▲), 500 rpm agitation, MBD sparging (●).

growth rate for the MBD-sparged and air-sparged fermentations at 500 rpm were almost identical because the DO level in both systems had exceeded the critical concentration and the specific growth rate was maximum.

The observed dry cell mass yield on substrate (0.43 g/g) for the MBD-sparged fermentation at 150 rpm was comparable to that of the air-sparged fermentation (0.53 g/g) at 500 rpm. The growth rate in the logarithmic phase for the two fermentations were almost identical (Fig. 4) and the specific growth rates were 0.52 h^{-1} and 0.56 h^{-1}, respectively, for the MBD-sparged fermentation at 150 rpm and air-sparged fermentation at 500 rpm. The DO levels for both systems were very high and well above the critical

Table 2
Power Consumption Estimated for 1-L Fermentation

Device consuming power	Power requirement ($kW \times 10^6$)			
	Air sparging @144 rpm	MBD sparging @144 rpm	Air sparging @476 rpm	MBD sparging @476 rpm
Agitator	63.70	63.70	2750	2750
Air compressor	14.55	14.55	14.55	14.55
MBD generator	—	21611	—	21611
Total	78.25	21689	2765	24376
Power per unit volume ($kW \times 10^6/L$)	78	21689	2765	24376

DO concentrations, hence the specific growth rates were near the maximum. The volumetric mass transfer coefficients were also very high and similar for both systems (Table 1).

Power Consumption

The total power consumption for each run was the sum of the power from the agitator, air compressor, and the MBD generator (the MBD motor, MBD delivery, and recycle pumps). The estimated power consumption for the 1-L fermentation is shown in Table 2. The highest power demand for the 1-L fermentation was from the MBD generator (motor, delivery, and recycle pumps). The coupling of the MBD unit to the conventional air-sparged system increased the power demand more than 200-fold when the fermentation was run at an agitation speed of 144 rpm. However, the observed cell mass yield on substrate (0.4 g/g) for the MBD-sparged fermentation at the low agitation speed (144 rpm) was only 1.5 times better than the conventional air sparged at 144 rpm. When the conventional air-sparged system's agitation speed was increased to 476 rpm, power consumption increased 35-fold and cell mass yield increased to 0.6 g/g. Comparing the MBD-sparged system at low agitation speed (144 rpm) to the conventional air-sparged fermentation at high agitation speed (476 rpm), the power consumed by the MBD system was eightfold higher than that consumed by the conventional air-sparged system. The observed mass yield (0.6 g/g) for the conventional air-sparged system at high agitation speed (476 rpm) was significantly ($p < 0.05$) higher than that obtained for the MBD-sparged system at 144 rpm. Thus, for small-scale fermentation, although there was a substantial increase in dry cell mass yield, the increased power consumption could not be justified. The lower than expected cell mass yield was attributed to the small working volume which resulted in low gas hold-up.

The power consumption in the 50-L fermentation is shown in Table 3. The power consumed at 150 rpm and 500 rpm using the MBD sparging was higher than that required for the corresponding air-sparged fermentation.

Table 3
Power Consumption Estimated for 50-L Fermentation

Device consuming power	Power requirement ($kW \times 10^6$)			
	Air sparging @150 rpm	MBD sparging @150 rpm	Air sparging @500 rpm	MBD sparging @500 rpm
Agitator	2030	2030	89820	89820
Air compressor	5380	5380	5380	5380
MBD generator	—	23150	—	23150
Total	7410	30560	95200	118350
Power per unit volume ($kW \times 10^6/L$)	148	611	1904	2367

However, the advantage of the MBD sparging can be seen by comparing the product yields from the two systems. At 150 rpm, the cell mass yield on substrate in the MBD-sparged fermentation is comparable to that obtained at 500 rpm using the air-sparged system. The specific growth rate of the MBD-sparged system was 91% of the maximum value (0.57 h^{-1}) estimated for the microorganism using the Hanes–Woolf plot *(23)* (Fig. 3B) while that for the 500-rpm air-sparged system was 98%. On the other hand, the power required per unit volume in the air-sparged system at 500 rpm was 1904×10^{-6} kW/L compared to 611×10^{-6} kW/L for the MBD-sparged fermentation. Clearly, there is a threefold reduction in power consumption in the MBD-sparged system for a similar biomass yield compared to the conventional air-sparged fermentation. The advantage of the MBD-sparged system on the larger-scale fermentation was probably because of the increased gas hold-up due to the larger working volume. Thus, a significant power saving can be realized using the MBD-sparged system for large-scale aerobic fermentation.

Conclusions

The use of the MBD sparging for aerobic fermentation has clearly demonstrated that dissolved oxygen concentration above the critical concentration can be attained at very low agitation rates. The scale-up of the MBD-sparged fermentation showed that some substantial benefits could be derived from using this technology in aerobic fermentation. For small-scale fermentation, although there were substantial increases in the dry cell mass production, the corresponding increase in power consumption to attain the increased biomass yield could not be justified. However, when the process was scaled-up, there was a threefold reduction in power consumption, and dry cell mass production increased, probably because of increased gas hold-up. Thus, we expect further improvements in cell mass growth yield and reduction in power consumption with further increases in reactor working volume.

References

1. Bailey, J. E. and Ollis, D. F. (1986), *Biochemical Engineering Fundamentals*, 2nd edition. McGraw-Hill Book Company, New York.
2. Kaster, J. A., Michelsen, D. L., and Velander, W. H. (1990), *Appl. Biochem. Biotechnol.* **24/25,** 469–484.
3. Bredwell, M. D. and Worden, R. M. (1998), *Biotechnol. Progress* **14,** 31–38.
4. Srivastava, P., Hahr, O., Buchholz, R., and Worden, R. M. (2000), *Biotechnol. Bioeng.* **70(50),** 525–532.
5. Sebba, F. (1985), An improved generator for micron-sized bubbles. *Chemistry and Industry*, February 4, 1985 pp. 91–92.
6. Sebba, F. (1987), *Foams and Biliquid Foams-Aphrons*. Wiley, Chichester, Chap 5.
7. Sebba, F. (1971), *J. Colloid Interface Sci.* **35(4),** 643.
8. Kaster, J. A. (1988), Increased oxygen transfer in a yeast fermentation using a microbubble dispersion. MS Thesis, Virginia Polytechnic Institute and State University, Blacksburg VA.
9. Oolman, T. O. and Blanch, H. W. (1983), Bubble coalescence and break-up in fermenters-effect of surfactant, inorganic salts, and non-Newtonian rheology. *Abstracts of Papers-American Chemical Society*.
10. Oolman, T. O. and Blanch, H. W. (1986), *Chem. Engin. Commun.* **43,** 237–261.
11. Karow, E. O., Bartholomew, W. H., and Sfat, M. R. (1953), *Agricultural Food Chem.* **1(4),** 302.
12. Miller, G. L. (1959), *J. Biol. Chem.* **31(3),** 426–428.
13. Hubbard, D. W., Ledger, S. E., and Hoffman, J. A. (1994), Scaling-up aerobic fermentation which produce non-Newtonian, viscoelastic broths, in *Advances in Bioprocess Engineering*, Galindo, E. and Ramirez, O. T. (eds.), Kluwer Academic, Boston, MA, pp. 95–101.
14. Hubbard, D. W. (1987), Scale-up strategies for bioreactors, in *Biotechnology Processes, Scale-Up and Mixing*, Ho, C. S. and Oldshue, J. Y. (eds.), American Institute of Chemical Engineers, New York, NY, pp. 168–184.
15. Wang, D. I. C., Cooney, C. L., Demain, A. L., Dunnill, P., Humphrey, A. E., and Lilly, M. D. (1979), *Fermentation and Enzyme Technology*, John Wiley, New York, pp. 157–193.
16. Mateles, R. I. (1971), *Biotechnol. Bioeng.* **13,** 581–582.
17. McCabe, W. L., Smith, J. C., and Harriot, P. (2001), *Unit Operations of Chemical Engineering*, sixth edition, McGraw-Hill, New York, NY pp. 238–285.
18. Oyama, Y. and Endoh, K. (1955), *Chem. Eng. (Japan)* **19,** 2–11.
19. Geankoplis, C. E. (1993), *Transport Processes and Unit Operations*, Prentice Hall, Englewood Cliffs, NJ, pp. 31–112.
20. Perry, R. H., Green, D. W., and Maloney, J. O. (eds.) (1984), *Perry's Chemical Engineers Handbook*, 5th edition, McGraw-Hill, New York, pp. 6–16.
21. Shuler, M. L. and Kargi, F. (1992), *Bioprocess Engineering, Basic Concepts*, Prentice Hall, Englewood Cliffs, NJ, pp. 148–198.
22. Ju, L.-K. and Chase, G. G. (1992), *Bioprocess Engin.* **8,** 49–53.
23. Shuler, M. L. and Kargi, F. (1992), *Bioprocess Engineering, Basic Concepts*, Prentice Hall, Englewood Cliffs, NJ, pp. 58–102.